



Membrane charge dependent states of the β -amyloid fragment A β (16–35) with differently charged micelle aggregates

Manuela Grimaldi^{a,1}, Mario Scrima^{a,1}, Cinzia Esposito^a, Giuseppe Vitiello^c, Anna Ramunno^a, Vittorio Limongelli^b, Gerardino D'Errico^c, Ettore Novellino^b, Anna Maria D'Ursi^{a,*}

^a Department of Pharmaceutical Sciences, University of Salerno, I-84084 Fisciano, Italy

^b Department of Pharmaceutical and Toxicological Chemistry, University of Naples "Federico II", I-80131 Naples, Italy

^c Department of Chemistry, University of Naples "Federico II", I-80131 Naples, Italy

ARTICLE INFO

Article history:

Received 1 October 2009

Received in revised form 8 December 2009

Accepted 16 December 2009

Available online 4 January 2010

Keywords:

Amyloid peptide

NMR spectroscopy

Micelle solution

EPR spectroscopy

Spin-labeled peptide

ABSTRACT

A β (16–35) is the hydrophobic central core of β -amyloid peptide, the main component of plaques found in the brain tissue of Alzheimer's disease patients. Depending on the conditions present, β -amyloid peptides undergo a conformational transition from random coil or α -helical monomers, to highly toxic β -sheet oligomers and aggregate fibrils. The behavior of β -amyloid peptide at plasma membrane level has been extensively investigated, and membrane charge has been proved to be a key factor modulating its conformational properties. In the present work we probed the conformational behavior of A β (16–35) in response to negative charge modifications of the micelle surface. CD and NMR conformational analyses were performed in negatively charged pure SDS micelles and in zwitterionic DPC micelles "doped" with small amounts of SDS. To analyze the tendency of A β (16–35) to interact with these micellar systems, we performed EPR experiments on three spin-labeled analogues of A β (16–35), bearing the methyl 3-(2,2,5,5-tetramethyl-1-oxypyrrolinyl) methanethiolsulfonate spin label at the N-terminus, in the middle of the sequence and at the C-terminus, respectively. Our conformational data show that, by varying the negative charge of the membrane, A β (16–35) undergoes a conformational transition from a soluble helical-kink-helical structure, to a U-turn shaped conformation that resembles protofibril models.

© 2009 Elsevier B.V. All rights reserved.

1. Introduction

Alzheimer's disease (AD) is a progressive neurodegenerative disorder and is the most common cause of dementia in adults. Mechanisms underlying this disease are still poorly understood,

but the deposition of senile plaques composed of fibrillar aggregates of amyloid β peptide (A β) is a characteristic hallmark of the pathology, and believed to play a fundamental role in disease pathogenesis [1–4]. The formation of amyloid aggregates is typical of numerous diseases: type 2 diabetes, Parkinson's disease, Huntington's disease and Creutzfeldt–Jacob disease [5,6]. Therefore the comprehension of the mechanism triggering the amyloid misfolding aggregation is critical for the development of therapies to treat all these diseases.

β -amyloid peptides are 39 to 43 amino acids long, derived from the proteolytic cleavage of amyloid precursor proteins (APP) by β - and γ -secretases. A β (1–40) and A β (1–42) are the main components of plaques found in the brain tissue of AD patients [7,8]. Depending on the conditions present, these peptides undergo a conformational transition from random coil or α -helical monomers to highly toxic β -sheet oligomers and aggregate fibrils [9–11].

A β (16–35) corresponds to the hydrophobic core of the β -amyloid peptide. It has been implicated in aggregation/disaggregation processes and it is the focus of attention in the search for peptide or peptidomimetic inhibitors of A β fibrillation [12–14]. The structural coordinates of β -amyloid fibrils pertain to this portion of the peptide [15]. In a recent model solved for A β (1–40) in complex with the phage-display selected affibody protein Z(Abeta3), [16] the hydrophobic core A β (17–36) was bound to the affibody in a β -hairpin

Abbreviations: A β , amyloid β peptide; APP, amyloid precursor proteins; Boc, *tert*-butyloxycarbonyl; CD, circular dichroism; CMC, critical micellar concentration; DCM, dichloromethane; DMF, *N,N*-dimethylformamide; DPC, dodecylphosphocholine; DQF-COSY, double quantum filtered correlation spectroscopy; 5-DSA, 5-doxylosteaic acid; 16-DSA, 16-doxylosteaic acid; EPR, electron paramagnetic resonance; ESI-MS, electrospray/ionization mass spectra; EtOAc, Ethyl acetate; Fmoc, 9-fluorenylmethyloxycarbonyl; HOBT, *N*-hydroxybenzotriazole; HPLC, high performance liquid chromatography; LiDS, lithium dodecyl sulfate; SLMTS, spin-label methyl 3-(2,2,5,5-tetramethyl-1-oxypyrrolinyl) methanethiolsulfonate; MTS, methyl 3-(2,2,5,5-tetramethyl-1-oxypyrrolinyl) methanethiolsulfonate label; MD, Molecular dynamics; NMM, *N*-methylmorpholine; NOE, nuclear Overhauser effect; NOESY, NOE Spectroscopy; RMSD, root mean square deviation; RP-HPLC, reversed phase HPLC; Rt, retention time; SDS, sodium dodecyl sulphate; SPPS, solid phase peptide synthesis; THF, Tetrahydrofuran; TBTU, 2-(1*H*-benzotriazol-1-yl)-1,1,3,3-tetramethyluronium tetrafluoroborate; TLC, thin-layer chromatography; TFA, trifluoroacetic acid; TEA, triethylamine; TOCSY, Total Correlated Spectroscopy

* Corresponding author. Medicinal Chemistry, Department of Pharmaceutical Sciences, University of Salerno, Via Ponte Don Melillo, 84084, Fisciano, Salerno, Italy. Tel./fax: +39 089 969748.

E-mail address: dursi@unisa.it (A.M. D'Ursi).

¹ These authors have contributed equally to this work.

conformation, providing the first high-resolution structure of A β in the β conformation [16].

In spite of a great deal of experimentation, the mechanisms favoring the formation of amyloid aggregates are unclear. As β -amyloid peptides are enzymatic products of the transmembrane protein APP, the implication of plasma membrane in β -amyloid conformational modification have been extensively investigated. Nevertheless, data collected up to now have been controversial and, to some extent, contradictory, depending in many cases on the methodology employed.

Increasing evidence, supported by experiments on several different amyloidogenic proteins, show that the membrane surfaces may act as a two-dimensional template for the formation of amyloid nucleation seeds [17–21] forming the senile plaques that are responsible for neuronal injury [22]. The structural behavior of non-fibril forming fragments of amyloidogenic proteins proved that plasma membrane is able to enhance the tendency to form aggregate: membrane surface may favor specific peptide secondary structures orienting the exposition of the sites that, on the peptide surface, are critical for the aggregation [23–29].

In a different hypothesis fibril-formation is not the main mechanism determining amyloid toxicity at membrane level. Instead of mature amyloid fibers, small oligomeric species of A β and other amyloid proteins [30] may be responsible for membrane destabilization, triggering the disruption of intracellular calcium homeostasis, which is a central event in the pathogenesis [26–28]. The targeting of compounds specifically to these oligomer toxic species, rather than to the final amyloid fibers, may be effective at reducing the toxicity of amyloidogenic proteins. Unfortunately, with the exception of few successful applications of pulsed field gradient (PFG) NMR spectroscopy, [31] the analysis of earlier oligomeric species is generally difficult due to the experimental limitations in characterizing unstable heterogeneous mixtures that contain a wide range of molecular sizes.

It is well known that the plasma membrane is an extremely complex bio-system. To analyze the effect of single plasma membrane components on the structural behavior of A β peptides, many studies have been carried out in membrane-mimicking models characterized by different complexities and compositions. All of these data, acquired with different biophysical techniques, point to the importance of membrane charge as a key factor in modulating the conformation of amyloid peptide and its ability to interact with the membrane surface. Specifically, the release of encapsulated dyes, [32] shifts of lipid head group, ^{31}P nuclear magnetic resonances (NMRs), [33–35] changes in bilayer fluidity [36] and monolayer studies [37–39] indicate that the structured A β is associated with anionic membranes. A β (1–40) binds negative electrostatically charged membranes, positioning itself on the outer envelope of the polar headgroup or in a transmembrane position. This electrostatic interaction is essential to stabilize the A β α -helical conformation and to prevent the release of the peptide from producing toxic aggregates [40].

The experiments described above, employed sophisticated membrane-mimicking models composed of highly compatible phospholipids; nevertheless although biologically relevant, they do not provide information at the atomic level regarding the structural changes of A β in response to fine adjustments of membrane charge.

High-resolution conformational data of A β peptide and its related fragments in membrane-mimicking systems have been produced, thanks to multidimensional NMR spectroscopy studies in detergent micelle solutions [41–46]. These are biophysical systems widely employed as lipid bilayer mimetic media in NMR studies of membrane proteins and polypeptides thanks to the rapid and effectively isotropic reorientation of the protein which enable high quality NMR experiments to be produced [47,48]. In reality, detergents are a more dynamic environment than the native bilayer and may impart flexibility and instability to the solubilized membrane protein,

possibly resulting in denaturation [49]. Therefore in the search for a membrane mimetic micelle system, detergents able to preserve the folding and the functionality of the protein should be selected. DPC micelles are considered good model to mimic the phospholipid membrane, since characterized by a headgroup identical to phosphatidylcholine, the most common lipid in animal cell membranes. Several studies have shown that DPC preserve the native conformations of membrane-associated peptides and enzyme activity of membrane proteins in some cases [50,51]. SDS are anionic detergents producing negatively charged micelles. SDS is known as denaturant of protein domains [52,53], but it is commonly employed in the identification of native helix–helix interactions in TM segments [54] and in some instances, is able to maintain the native tertiary and quaternary structure of membrane proteins that lack significant extramembranous domains [55].

SDS and DPC micelles have been used to solve the NMR structure of full length A β peptide and its related fragments [41–46]. In SDS micelle solution, A β (1–40) has been shown to assume an α -helical structure within residues 15–24 and 28–36, having a kink or hinge around residues G25–N27. The peptide has a bent shape and is thought to be partly inserted into the micelle. In lithium dodecyl sulfate (LiDS) or SDS micelles, the shorter fragments A β (12–28), A β (25–35) and A β (1–28) all form α -helical structures [44,45]. In pure SDS and pure DPC lipid environments the interaction of A β (12–28) with zwitterionic DPC micelles was shown to be weak. In contrast, the interaction of the peptide with anionic SDS micelles was strong [46]. Multidimensional NMR was used to analyze ganglioside–A β interactions in SDS micelles and to study Italian and Flemish variants of A β (11–28) [56–58].

SDS and DPC micelles are respectively characterized by strongly negative and completely zwitterionic surfaces. Considering the sensitivity of the A β peptide to membrane charge, we hypothesize that a drastic change, from a strongly negative SDS surface to a zwitterionic DPC surface, may not be necessary to induce conformational modifications of A β peptides. More moderate changes of charge contents, such as those produced by mixed negatively charged and zwitterionic detergent micelles, may be sufficient. Mixtures of DPC “doped” with small amounts of SDS are known to be efficacious toward modulating the charge distribution of the micelle surface [59]. Therefore, we undertook a comparative conformational study, by means of CD and NMR spectroscopy, of the β -amyloid fragment A β (16–35) in negatively charged pure SDS micelles and in DPC/SDS 90/10 (w:w) mixed micelles. The tendency of A β (16–35) to interact with these micellar systems was analyzed by electron paramagnetic resonance (EPR) spectroscopy [60]. In the present work, we performed two complementary series of EPR experiments by randomly including spin-labeled peptides and spin-labeled lipids in micelle aggregates. Three spin-labeled analogues of A β (16–35), bearing the MTSL spin label at the N-terminus, in the middle of the sequence and at the C-terminus (Fig. 1), were synthesized (see [Experimental section](#)) to monitor specific portions (N-terminus, C-terminus and middle of the sequence) of A β (16–35) at the micelle interface using EPR spectroscopy. The information obtained through these experiments was combined with those derived from spin-labeled micelles, yielding a detailed picture of A β (16–35)–micelle interactions.

Our conformational data show that, by varying the content of negative charges, A β (16–35) undergoes a conformational transition from a soluble helical–kink–helical structure, which is similar to others solved in analogue micelle systems, to a conformation that resembles protofibril models.

Interestingly, the A β (16–35) model in mixed micelles is similar to the first soluble strand–turn–strand conformation found for A β (1–40) in the affibody-complex. This conformational change is also reflected in changes of peptide mobility at the membrane interface.

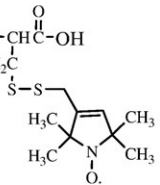
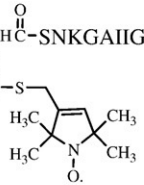
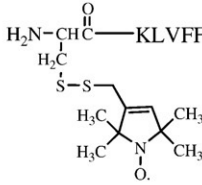
Aβ (16-35) Amyloid Peptide and the MTSL labeled derivatives	Name
KLVFFAEDVGSNKGAIIGLM	A β (16-35) (I)
$\text{KLVFFAEDVGSNKGAIIGLM}-\text{N}-\overset{\text{H}}{\underset{\text{H}_2\text{C}}{\text{C}}}-\overset{\text{O}}{\parallel}{\text{C}}-\text{OH}$ 	A β (16-35)-MTSLCterm (II)
$\text{KLVFFAEDV}-\text{N}-\overset{\text{H}}{\underset{\text{H}_2\text{C}}{\text{C}}}-\overset{\text{O}}{\parallel}{\text{C}}-\text{SNKGAIIGLM}$ 	A β (16-35)G25C-MTSL (III)
$\text{H}_2\text{N}-\overset{\text{O}}{\parallel}{\text{C}}-\text{KLVFFAEDVGSNKGAIIGLM}$ 	A β (16-35)-MTSLNterm (IV)

Fig. 1. Aminoacid sequence of A β (16–35) (I), A β (16–35) bearing MTSL spin label at the C-terminus (II), in the middle of the sequence (III) and at the N-terminus (IV).

In view of the fact that A β (16–35) is the hydrophobic core of the full length A β (1–42), a critical region in the aggregation-disaggregation processes, we can conclude that the solution structures of A β (16–35), in SDS pure micelles and in DPC/SDS mixed micelles, may be more generally considered models of two A β conformational states (soluble and protofibrillar). These are potentially useful as molecular targets in the search for molecules that act to prevent and/or reverse fibril aggregation.

2. Experimental section

2.1. Materials

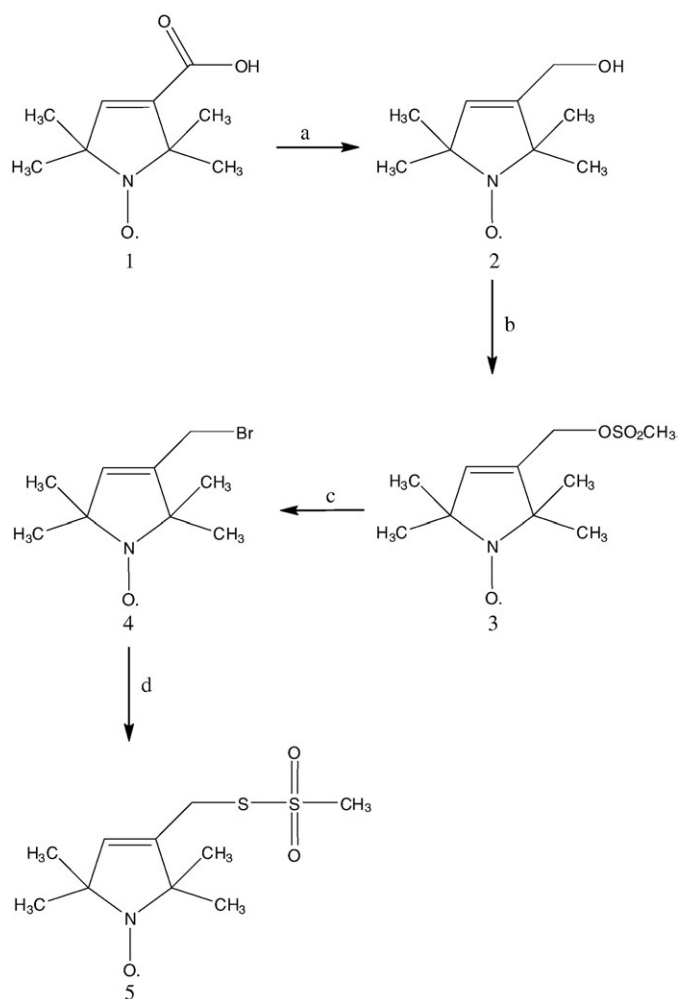
The starting material for the synthesis of **5** (Scheme 1), 2,2,5,5-tetramethyl-1-oxopyrrolidine-3-carboxylic acid, was purchased from Acros Organics. Protected amino acids and chemicals were purchased from Fluka. All other reagents and solvents were purchased from Sigma-Aldrich. Dry solvents were distilled under nitrogen immediately prior to use. Tetrahydrofuran (THF) was distilled from Na/benzophenone ketyl, while CH₂Cl₂ and triethylamine (TEA) were distilled from CaH₂. All intermediates (**1–4**) and the title compound (**5**) were purified by flash chromatography (silica gel 60, 230–400 mesh, Merck) using a mixture of EtOAc/petroleum ether (90/10 for **1–4** and 65:35 for **5**) as the eluent. Reaction and product mixtures were routinely monitored by thin-layer chromatography (TLC) on silica gel pre-coated F₂₅₄ Merck plates. Melting points were taken on a Gallenkamp melting point apparatus and were consistent with previously reported values [61–65]. Mass spectra of compound **5**

and labeled peptides A β (16–35)-MTSL^{C-term}, A β (16–35)G25C-MTSL and A β (16–35)-MTSL^{N-term} were obtained by electrospray ionization (ESI).

2.2. Solid-phase peptide synthesis and purification

A β (16–35) (K-L-V-F-F-A-E-D-V-G-S-N-K-G-A-I-I-G-L-M) and the analogous **II**, **III**, and **IV** (Fig. 1) were synthesized according on a manual batch synthesizer (PLS 4 \times 4, Advanced ChemTech) using a Teflon reactor (10 mL), applying the Fmoc/tBu solid phase peptide synthesis (SPPS) procedure. The Wang resin was swelled with DMF (1 mL/100 mg of resin) for 3 h before use.

Stepwise peptide assembly was performed by repeating for each added amino acid the following deprotection–coupling cycle: 1) Swelling: DMF (1 mL/100 mg of resin) for 5 min; 2) Fmoc-deprotection: resin is washed twice with 20% piperidine in DMF (1 mL/100 mg of resin, one wash for 5 min followed by another wash for 20 min); 3) Resin-washings: DMF (3 \times 5 min); 4) Coupling: scale employing HBTU/HOBt/NMM (2.5:2.5:3.5 eq.) as the coupling system and 2.5 eq. of the Fmoc protected amino acids. Each coupling was monitored by Kaiser test⁴³ and was negative, therefore recouplings were not needed; 5) Resin-washings: DMF (3 \times 5 min) and DCM (1 \times 5 min). After deprotection of the last NR-Fmoc group, the peptide resin was washed with methanol and dried *in vacuo* to yield the protected peptide-Wang-resin. The protected peptide was cleaved from the resin by treatment with TFA/H₂O/phenol/ethanedithiol/thioanisole (reagent K) (82.5:5:5:2.5:5 v/v) at a ratio of 10 mL to 0.5 g of resin at room temperature for 3 h. After filtration of the exhausted



Scheme 1. Reagents and conditions: a) LiAlH_4 , dry THF, rt, overnight (40%); b) $\text{CH}_3\text{SO}_2\text{Cl}$, dry CH_2Cl_2 , TEA, rt, 3 h (76%); c) LiBr, dry acetone, reflux, 3 h (71%); d) $\text{CH}_3\text{SO}_2\text{SNa}$, absolute EtOH, reflux, 4 h (80%).

resin, the solvent was concentrated *in vacuo* and the residue was triturated with ether.

The crude peptide was purified by preparative reversed phase high performance liquid chromatography (HPLC) using a Jupiter [Phenomenex, Anzola Emeilia (BO), Italy] C18 column (25×4.6 cm, 5μ , 300 Å pore size). The column was perfused at a flow rate of 3 mL/min with a mobile phase containing solvent A (0.1% TFA in water). A linear gradient from 50% to 90% of solvent B (acetonitrile in 0.1% TFA) for 40 min was adopted for peptide elution. The pure fraction was collected to yield a white powder after lyophilization. The molecular weight of the compound was determined by mass spectral analysis.

2.3. Mass spectral analysis

Peptide fragments were characterized using a Finnigan LCQ-Deca ion trap instrument equipped with an electrospray source (LCQ Deca Finnigan, San Jose, CA, USA). The samples were directly infused into the ESI source using a syringe pump set at a flow rate of $5 \mu\text{L}/\text{min}$. Data were analyzed with Xcalibur software.

2.3.1. Synthesis of spin-label methyl 3-(2,2,5,5-tetramethyl-1-oxypyrrolinyl) methanethiolsulfonate (SLMTS)

Spin-label methyl 3-(2,2,5,5-tetramethyl-1-oxypyrrolinyl) methanethiolsulfonate (SLMTS; **5**) was synthesized as shown in Scheme 1. According to previously reported procedures [44–47], alcohol **2** was

obtained by reduction with lithium aluminum hydride of commercially available 2,2,5,5-tetramethyl-1-oxypyrrolidine-3-carboxylic acid (**1**). Alcohol **2** was then reacted with methanesulfonyl chloride, followed by treatment with lithium bromide, to give the bromomethyl derivative (**4**). Finally, nucleophilic substitution of **4** with sodium methanethiosulfonate afforded the title compound as a brown solid in good yield.

2.4. Derivatization of $\text{A}\beta$ (16–35) with MTSL

To insert MTSL on the $\text{A}\beta$ (16–35) C-terminus, in the middle of the sequence and at the N-terminus, $\text{A}\beta$ (16–35) analogues were synthesized. These included the Cys residue at C-, in the middle (M-) and at the N-terminus to produce peptides **II**, **III**, and **IV**, respectively (Fig. 1).

Crude peptides **II**, **III**, or **IV** (1 eq) in $\text{CH}_3\text{CN}/\text{H}_2\text{O}$ (8:2; 4 mL) were incubated with a 4-fold molar excess of (1-oxyl-2,2,5,5-tetramethylpyrrolidin-3-yl)methyl methanesulfonate (**5**) in acetone (2 mL). The resulting mixture was stirred at room temperature for 72 h. Solvent was then removed by filtration and the residue was washed with ethyl ether until no appreciable amount of spin-label (**4**) was detected with TLC (EtOAc/petroleum ether 65:35). The purification of labeled peptides, designated as $\text{A}\beta$ (16–35)C-term or $\text{A}\beta$ (16–35)N-term, was achieved using a semi-preparative RP-HPLC C-18 bonded silica column. Purified peptides were determined by mass spectral analysis. Prior to EPR analysis, the peptides [$\text{A}\beta$ (16–35)-MTSL^{C-term}, $\text{A}\beta$ (16–35)G25C-MTSL, and $\text{A}\beta$ (16–35)-MTSL^{N-term}] were treated with 10% aqueous ammonia (pH 9.5) for 4 h at room temperature, to re-oxidize the spin label back to the nitroxide form [66].

2.5. Sample preparation for CD and NMR analysis

Unstructured aggregates are often present in untreated samples from synthesis experiments and can severely hamper solubility. To disaggregate such material, which could have been present in the dry peptide, all CD and NMR samples were treated with TFA immediately before being dissolved in the final mixture, as described by Jao et al. [67].

To record CD and NMR experiments in water solution, $\text{A}\beta$ (16–35) that was previously treated according to the procedure reported above, [67] was added to an aqueous solution (pH 5.4 phosphate buffer). This yielded final concentrations of 0.15 mM (CD experiments) and 1.5 mM (NMR experiments). For NMR samples, a $\text{H}_2\text{O}/\text{D}_2\text{O}$ (90:10 v/v) mixture was used.

The samples for CD and NMR experiments in SDS micelles were prepared by dissolving $\text{A}\beta$ (16–35) peptide (0.15 mM for CD experiments and 1.5 mM for NMR experiments) in a SDS/water mixture. A concentration of 80 mM SDS was used, which is 10 times higher than the SDS critical micellar concentration (cmc) [68]. The final pH was adjusted to 5.4 using 20 mM of phosphate buffer. For NMR experiments, d^{25}SDS was used.

Owing to solubility issues, SDS titrations were carried out for CD and NMR studies in DPC/SDS mixed micelles. An appropriate amount of $\text{A}\beta$ (16–35) (see above) was dissolved in a DPC/ H_2O mixture. The DPC concentration used was 27 mM (27 times higher than DPC cmc) [68]. Subsequently, titration with SDS was carried out to cover the molar DPC:SDS ratio of 90/10 (27 mM/3 mM) and to reproduce the partial (2–3%) negative charge present in the typical membrane of eukaryotic cells [69]. The final pH was adjusted to 5.4 using 20 mM of phosphate buffer. For NMR experiments, d^{25}SDS and d^{38}DPC were used.

2.6. CD analysis

All CD spectra were recorded using a JASCO J810 spectropolarimeter at room temperature and with a cell path length of 1 mm. CD

spectra were performed at 25 °C using a measurement range from 260 to 190 nm, 1 nm band width, 4 accumulations, and 10 nm/min scanning speed. Spectra were corrected for solvent contribution.

For an estimation of secondary structure content, CD spectra were analyzed using the SELCONN algorithm from the DICHROWEB website [70,71].

2.7. NMR analysis

NMR spectra were collected using a Bruker DRX-600 spectrometer at 300 K. One-dimensional (1D) NMR spectra were recorded in the Fourier mode with quadrature detection. The water signal was suppressed by low-power selective irradiation in the homo-gated mode. DQF-COSY, TOCSY, and NOESY [72–74] experiments were run in the phase-sensitive mode, using quadrature detection in ω_1 , via time-proportional phase increases of the initial pulse. Data block sizes were 2048 addresses in t_2 and 512 equidistant t_1 values. Prior to Fourier transformation, the time domain data matrices were multiplied by shifted \sin^2 functions in both dimensions. A mixing time of 70 ms was used for the TOCSY experiments. NOESY experiments were run with mixing times in the range of 100–250 ms. Qualitative and quantitative analyses of DQF-COSY, TOCSY, and NOESY spectra were achieved using SPARKY software [75].

2.8. Structure refinement using molecular dynamics calculations

Peak volumes were translated into upper distance bounds with the CALIBA routine from the DYANA software package [76]. The requisite pseudoatom corrections were applied for non-stereospecifically assigned protons at prochiral centers and for the methyl group. After discarding redundant and duplicated constraints, the final list of constraints (Table 1) was used to generate an ensemble of 100 structures by the standard DYANA protocol of simulated annealing in torsion angle space implemented (using 6000 steps). No dihedral angle restraints and no hydrogen bond restraints were applied. The best 20 structures, which had low target function values (0.83–1.19) and small residual violations (maximum violation = 0.38 Å), were refined by in vacuo minimization in the AMBER 1991 force field using the SANDER program of the AMBER 5.0 suite [77,78]. To mimic the effect of solvent screening, all net charges were reduced to 20% of their real value. Moreover, a distance-dependent dielectric constant ($\epsilon = r$) was used. The cut-off for non-bonded interactions was 12 Å. NMR-derived upper bounds were imposed as semi-parabolic penalty functions, with force constants of 16 kcal/mol Å². The function was shifted to be linear when the violation exceeded 0.5 Å. The best 10

structures after minimization had AMBER energies ranging from –441.4 to –391.1 kcal/mol. Final structures were analyzed using the Insight 98.0 program (Molecular Simulations, San Diego, CA, USA).

2.9. EPR spectroscopy

Two series of EPR experiments were performed. For the former experiment, spin-labeled peptides, including A β (16–35)-MTSL^{C-term}, A β (16–35)G25C-MTSL, or A β (16–35)-MTSL^{N-term} (II, III, and IV, respectively, in Fig. 1), were dissolved in the appropriate amount of aqueous buffer or micellar solution to obtain a 0.2 mM peptide concentration. The peptide/surfactant molar ratio was set to 1:100. Thus, in these experiments, the effect of micelles on the EPR spectrum of labeled peptides was observed. In the latter series of measurements, the spin probes 5-doxylstearic acid and 16-doxylstearic acid (5-DSA and 16-DSA, respectively; Sigma) were inserted into micellar aggregates at a 1:100 probe/surfactant mole ratio (surfactant concentration 20 mM). The effect of unlabeled peptides A β (16–35), at a 1:10 peptide/surfactant mole ratio, on their EPR spectrum was monitored. In both series of experiments, the samples were deoxygenated and successively sealed in 1.00 mm i.d. quartz capillaries in a nitrogen atmosphere. EPR spectra were obtained using a Bruker ELEXYS e500 X-band spectrometer. Instrumental parameters were as follows: modulation amplitude = 0.16 G, to avoid signal over modulation; time constant = 1.28 ms; receiver gain = 60 dB; and microwave power = 2 mW (20 dB), to prevent saturation effects. All measurements were performed at room temperature.

3. Results

3.1. CD spectroscopy

The conformational preferences of A β (16–35) were preliminarily screened by CD spectroscopy. Fig. 2 shows the CD spectra of A β (16–35) recorded in water, in pure SDS micelles, and in DPC/SDS mixtures at 90/10 M/M (molar ratio). The CD spectrum recorded in aqueous solution at pH 5.4 indicates the prevalence, in this medium, of disordered structures. CD spectra of A β (16–35) acquired in pure SDS micelles evidence positive ellipticity value at 198 nm and two minima at 208 and 222 nm, which are suggestive of helical conformations. CD spectra recorded in DPC/SDS mixed micelle solutions showed a pronounced negative ellipticity value at 218 nm. The quantitative evaluation of

Table 1

Structural statistics for the final 20 structures A β (16–35) in SDS and in DPC/SDS micelles.

PARAMETER	A β (16–35) in SDS micelles	A β (16–35) in DPC/SDS micelles	
RMSD from mean structure (Å)	Peptide region		
	18–24 24–28 28–35	0.4285	0.5420
NOE distance restraints	Total	194	221
	Intra	66	70
	Short	83	90
	Medium	45	59
	Long	0	2
Ramachandran plot	Residues in most favored regions	56.3%	29.7%
	Residues in additional allowed regions	28%	47.3%
	Residues in generously allowed regions	14.7%	23%

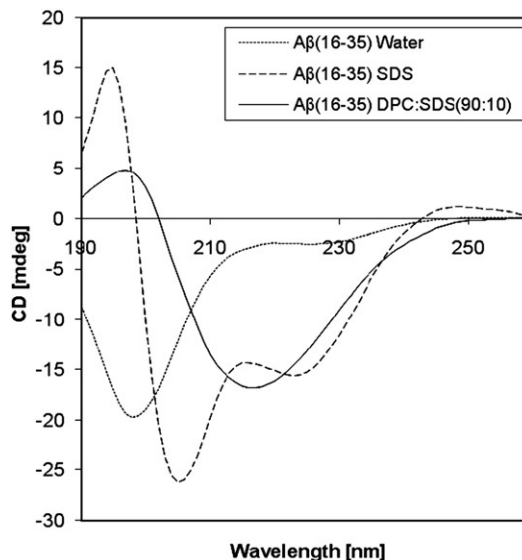


Fig. 2. CD spectra of A β (16–35) recorded in water, in pure SDS micelles and in DPC/SDS mixtures at 90/10 M/M.

mentioned CD curves, which was performed using the DICHROWEB [70,71] interactive website (SELCONN algorithm), indicates that A β (16–35) in water solution assumes random coil conformations with minimal amounts of turn and strand structures. In pure SDS micelles, this assumes 60% helical, 30% β -turn, and 10% random coil conformations. In mixed DPC/SDS micelles, A β (16–35) is present as 30% helical, 25% β -turn, 10% β -strand, and 35% random coil conformations.

3.2. NMR spectroscopy

3.2.1. Chemical shift analysis

A whole set of 1D and 2D proton spectra were recorded in water, in pure SDS micelles, and in mixed DPC/SDS micelles. To check the absence of self-aggregation, spectra were acquired in the peptide concentration range of 0.5–15 mM. No significant changes were observed in the distribution and shape of ^1H resonances, indicating that no aggregation phenomena occurred in this concentration range. Complete assignments of the proton spectra of A β (16–35) in water and micellar environments (see [Supplementary material](#)) were achieved by the standard Wüthrich [79] procedure. Analysis of 2D spectra was performed using the SPARKY software package [75].

Fig. 3 reports a graphical representation of the proton CH α chemical shifts differences of A β (16–35) in SDS and DPC/SDS micelles, and the CH α values of random coil peptides [79].

CH α chemical shifts are known to be diagnostic of peptide and protein secondary structures. According to the Chemical Shift Index (CSI), [80] groups of four (not necessarily consecutive) CH α showing >0.1 ppm upfield shifted values, as compared to random coil values, are diagnostic of helix conformations. Regions characterized by non-consecutive CH α values close or low-field shifted, as compared to the CH α random coil values, are diagnostic of coil conformations [80]. In agreement with this analysis, CH α chemical shift difference trends were different overall for A β (16–35) in SDS and DPC/SDS micelle solutions. This indicates a generally different secondary structure of the peptide for the two micelle conditions. Numerous CH α upfield shifts for A β (16–35) in SDS demonstrate evidence for the appreciable presence of peptides in turn–helical conformations. Whereas, CH α chemical shift differences for A β (16–35) in DPC/SDS (90/10 M/M) are diagnostic of low ordered structures. Specifically, the most significant divergences were observed for residues V24, G25, N27, I31, and I32.

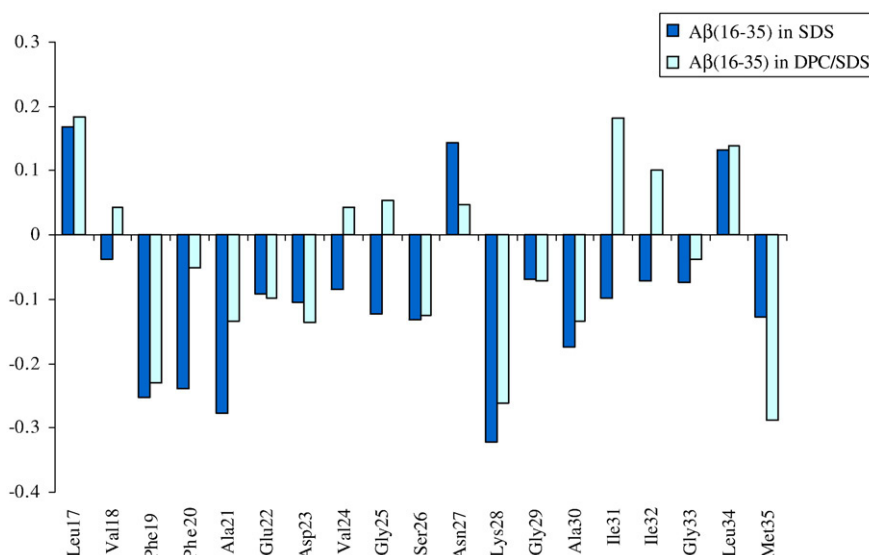


Fig. 3. CH α chemical shifts differences of A β (16–35) in SDS (blue) and DPC/SDS (cyan) micelles, and the CH α values of random coil peptides.

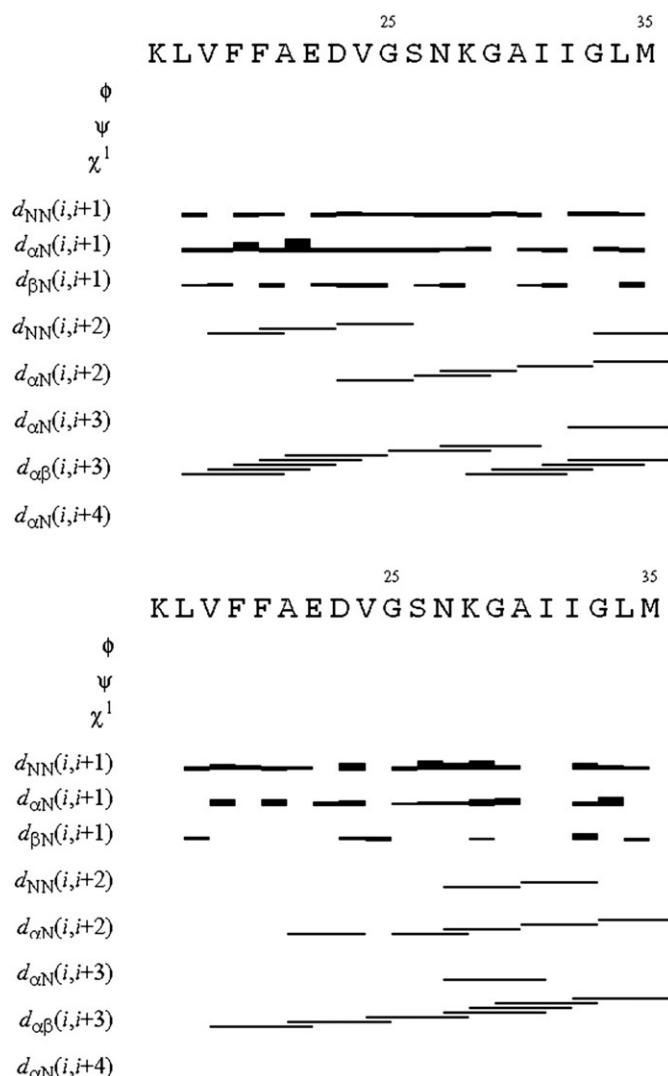


Fig. 4. NOE connectivities of A β (16–35) NOESY spectra in pure SDS micelles (top), and in DPC/SDS 90/10 M/M mixed micelles (bottom).

3.3. NMR structure calculation

Fig. 4 shows the NOE connectivities of A β (16–35) NOESY spectra in water, in pure SDS micelles, and in DPC/SDS mixed micelles. Sporadic sequential NH–NH(*i*, *i* + 1), medium range CH α –CH $_2$ β (*i*, *i* + 3), and CH α –NH(*i*, *i* + 2) NOE effects were observed in the NOESY spectrum of A β (16–35) in water. These involved, in particular, segment N27–L34, suggesting the presence of a nascent helical structure in this portion of the peptide. The lack of regular NOE patterns in the remaining part of the peptide suggests the absence of any regular secondary structure.

In pure SDS micelles, sequential NH–NH(*i*, *i* + 1) effects involved all residues of the L17–L34 sequence. Regular CH α –CH $_2$ β (*i*, *i* + 3) were present in segments L17–G25 and K28–M35, respectively. Additionally, sporadic CH α –NH(*i*, *i* + 2) and NH–NH(*i*, *i* + 2) NOE effects were observed along different triads of the sequence.

In DPC/SDS mixed micelles, the NOE pattern was less regular, as compared to that observed in SDS pure micelles. Several regular NH–NH(*i*, *i* + 1) and CH α –CH $_2$ β (*i*, *i* + 3) medium range connectivities were observed.

The structural calculations of A β (16–35) in water, pure SDS micelles, and mixed DPC/SDS micelles were carried out using DYANA software on the basis of NOE data. This data was transformed into interprotonic distances and imposed as restraints in the calculation. Among 50 calculated structures, the resulting best twenty were selected according to the lowest values of their target functions. They were subjected to further minimization procedures with the SANDER module of AMBER 5.0 software, [77,78] using DYANA-derived restraints.

Fig. 5 shows NMR structure bundles of A β (16–35) in SDS and DPC/SDS micelles. Statistical information for the structural ensemble of A β (16–35) in water, SDS, and DPC/SDS micelles is shown in Table 1.

Analysis of the bundles, according to the PROCHECKNMR [81] procedure, indicated that A β (16–35) NMR structures in water were characterized by a turn-helical conformation on residues K28–M35. Ramachandran plots of A β (16–35) NMR structures in pure SDS micelles showed that the dihedral angles of different conformers were in good agreement and fell in allowed regions for residues L17–V24 and N27–M35 (Supplementary material). The scattering of dihedral angles in residues G25 and S26 was evident, indicating high structural flexibility at this point of the sequence (see Supplementary material). Analysis of the structure bundle, according to Kabsh and Sanders parameters, points to the presence of regular α -helical and type I β -turn conformations involving the residues F19–V24 and K28–I32, respectively. The conformation of fragment F19–V24 was stabilized by the presence of H-bonds involving NH A21 C O V18, NH E22 C O F19, NH E22 C O F20, and NH D23 C O F19. On the other hand,

the conformation of segment 28–32 was stabilized by the presence of H-bonds involving NH G29 C O N27 and NH I32 C O A30.

Ramachandran plots of A β (16–35) NMR structures in DPC/SDS micelles (see Supplementary material) demonstrated evidence of a general agreement among the dihedral angles of different conformers. With the exception of those belonging to C-terminal residues L34 and M35, all of them fall within allowed regions. For residues G25 and S26, low scattering of the dihedral angles was evident, as compared to the structures in pure SDS micelles. Evaluation of the structure bundle, according to Kabsh and Sanders parameters, points to the presence of regular type I β -turn structures, corresponding to the residues S24–N27. Several conformers showed an extension of the turn structures to segments F20–V24, or alternatively to K28–A30.

3.4. Complementary NMR and EPR spin-label aided studies

To investigate the positioning of A β (16–35) peptide relative to the surface and interior of micelles, we performed EPR and NMR experiments in the presence of spin-labeled substances (i.e. substances with unpaired electrons) [60,82,83]. We performed two complementary series of EPR experiments. In the first, spin-labeled peptides (Fig. 1) were used, enabling us to monitor how the presence of micelles affects peptide behavior. In the second series of experiments, we used micellar aggregates randomly labeled via the inclusion of small amounts of lipids bearing a radical group. In both cases, cyclic nitroxides were used as spin labels due to their remarkable stability and to the localization of the spin density on the NO moiety, which allows to extract a great deal of information on the label solubilization site from the EPR spectrum. Indeed, because of the coupling between the electron spin and the nuclear spin of the nitrogen atom, the EPR spectrum of a cyclic nitroxide presents three lines (see Fig. 6). The spacing between them corresponds to the nitrogen isotropic hyperfine coupling constant, A_N , which increases with the polarity of the medium in which the nitroxide is embedded. Furthermore, a detailed analysis of the lines' amplitudes allows to obtain the nitroxide correlation time, τ_C , which depends on the label rotational mobility, as determined by the microenvironment viscosity and/or by specific interactions. From a qualitative viewpoint, narrow lines (low τ_C) indicate that the label is quite free to rotate, while broad lines (high τ_C) indicate that the motional freedom is reduced. Broadening is usually much more evident for the line at high field [84].

A β (16–35) was properly spin-labeled at the C-terminus, in the middle of the sequence (position 25), and at the N-terminus, to produce A β (16–35)-MTSL^{C-term} (II), A β (16–35)G25C-MTSL (III), and A β (16–35)-MTSL^{N-term} (IV), respectively (Fig. 1). EPR spectra of all

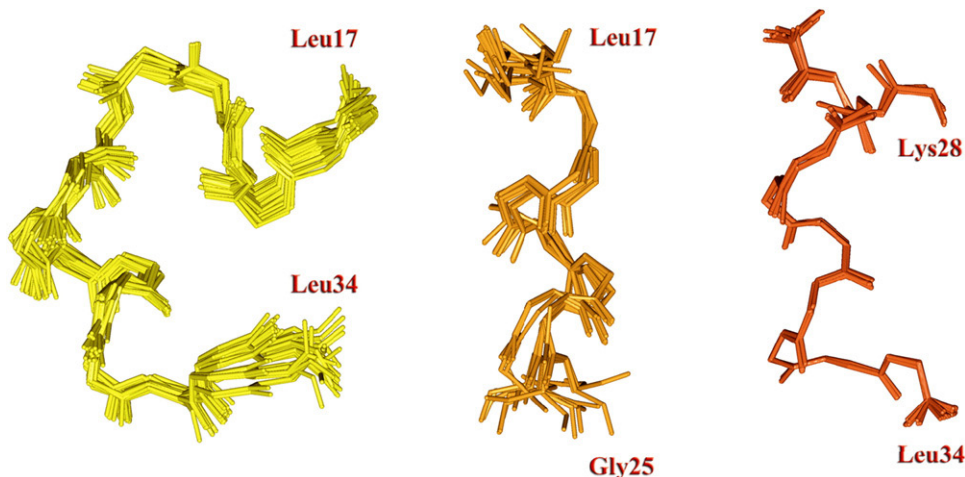


Fig. 5. NMR structure bundles of A β (16–35) in SDS micelles (segment 17–25—orange; segment 28–34—orange red) and in DPC/SDS micelles 90/10 M/M (yellow).

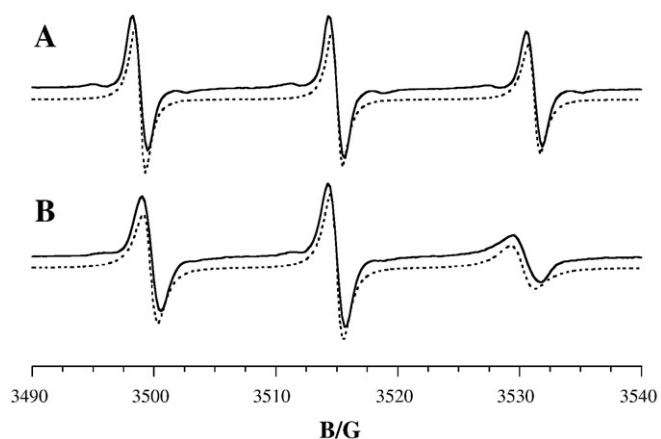


Fig. 6. Experimental (continuous line) and simulated (dotted line) EPR spectra of A β (16–35), labeled at the C-terminus, in phosphate buffer (A) and in SDS solution (B).

spin-labeled peptides were acquired in phosphate buffer, SDS, and DPC/SDS (90:10) micellar solutions. In all cases, the expected three hyperfine lines were observed. This is evidence that no peptide self-aggregation took place. If this were the case, then spin–spin interactions would have provoked the collapse of the three lines, i.e., the appearance of a single very broad line [85].

Furthermore, in all the systems considered here, EPR spectra showed narrow lines indicative of an isotropic fast motion. This is despite the fact that a slight, but significant broadening, due to the interaction between spin-labeled peptides and micelles, was evident (see spectrum B in Fig. 6 with respect to spectrum A). Consequently, spectral analysis was carried out according to the classical theory of motional narrowing for EPR lines [86].

A_N and τ_C values for A β (16–35)-MTSL^{C-term} (II), A β (16–35)G25C-MTSL (III) and A β (16–35)-MTSL^{N-term} (IV) in the various systems analyzed in the present work are shown in Table 2.

Table 2

Nitrogen coupling constant, A_N , and spin label correlation time, τ_C , measured by EPR experiments on either spin labeled A β (16–35) in phosphate buffer, SDS and DPC/SDS micelles or doxyl stearic acids in SDS and DPC/SDS micelles, in the absence and in the presence of A β (16–35).

	A_N /G	$\tau_C \times 10^{10}$ /s
<i>Aβ (16–35)Cterm</i>		
phosphate buffer	16.19 \pm 0.02	1.8 \pm 0.2
SDS	15.32 \pm 0.02	3.3 \pm 0.3
DPC/SDS 90:10	16.10 \pm 0.02	3.2 \pm 0.3
<i>Aβ (16–35)Nterm</i>		
phosphate buffer	16.20 \pm 0.02	1.7 \pm 0.2
SDS	15.81 \pm 0.02	2.8 \pm 0.3
DPC/SDS 90:10	15.68 \pm 0.02	3.1 \pm 0.3
<i>Aβ (16–35)G25C-MTSL</i>		
phosphate buffer	16.21 \pm 0.02	1.7 \pm 0.2
SDS	15.26 \pm 0.02	3.7 \pm 0.3
DPC/SDS 90:10	15.92 \pm 0.02	4.2 \pm 0.3
<i>5-DSA</i>		
SDS	15.07 \pm 0.04	17 \pm 2
SDS-A β (16–35)	14.96 \pm 0.04	28 \pm 3
DPC/SDS 90:10	14.48 \pm 0.04	27 \pm 3
DPC/SDS-A β (16–35)	14.39 \pm 0.04	30 \pm 3
<i>16-DSA</i>		
SDS	15.15 \pm 0.04	6.7 \pm 0.6
SDS-A β (16–35)	15.09 \pm 0.04	12.8 \pm 1.3
DPC/SDS 90:10	14.68 \pm 0.04	10.5 \pm 1.0
DPC/SDS-A β (16–35)	14.74 \pm 0.04	10.7 \pm 1.1

In phosphate buffer, no difference was found between values for the three spin-labeled peptides. Thus, the environment in which the nitroxide label is embedded did not depend on its positioning along the peptide chain, indicating that the whole molecule was fully exposed to the aqueous medium. Overall, significant changes in the EPR parameters, owing to the presence of SDS or DPC/SDS micelles, were evident. Particularly, the τ_C value increased, a consequence of a decrease in the label mobility. This evidence indicates peptide interactions with the micellar aggregates to occur. The whole peptide was involved in the interaction, as the three spin-labeled peptides showed comparable τ_C changes, even though a slightly higher τ_C increase was found for A β (16–35)G25C-MTSL.

At the same time, the decrease in A_N indicates that spin labels were embedded in a less polar microenvironment with respect to the aqueous medium. Specifically, as far as DPC/SDS micelles are considered, the extent of the A_N reduction is quite low (from 0.1 to 0.5 G) for all the three spin-labeled peptides. A comparable A_N reduction was reported in the literature for labels whose solubilization site in the micelles is just below the external hydrophilic layer [87]. Consequently, our evidences suggest a shallow insertion of the whole peptide in the mixed micellar aggregates (see Fig. 7 for a schematic representation of peptide–micelle relative positioning). In contrast, A β (16–35)-MTSL^{C-term} (II) and A β (16–35)G25C-MTSL (III) presented a more pronounced A_N decrease in SDS micelles (\sim 1 G). This suggests deep penetration of the second half of the A β (16–35) sequence in the SDS micellar apolar core, with the N-terminus being more exposed to the external medium (see Fig. 7).

To see whether the interaction with A β (16–35) influenced the microstructure of SDS and DPC/SDS (90:10) micelles, we performed EPR measurements on micellar solutions in the presence and absence of the peptide. Spin labels used for this experiment were 5-doxylstearic acid (5-DSA) and 16-doxylstearic acid (16-DSA). The former provided information on the micellar layer just below the external surface, while the latter gave information on the interior of the micellar hydrophobic core. Spectroscopic parameters obtained from these spectra are shown in Table 2. In both micellar systems, the τ_C value was higher for 5-DSA than for 16-DSA. In other words, the motion of 5-DSA was slower than for 16-DSA. This indicates a flexibility increase in segmental chain mobility when going from surfactant polar headgroups to the inner hydrophobic core of micelles. The presence of A β (16–35) caused significant effects on SDS micelles. In fact, for both spin-labeled surfactants, τ_C significantly increased.

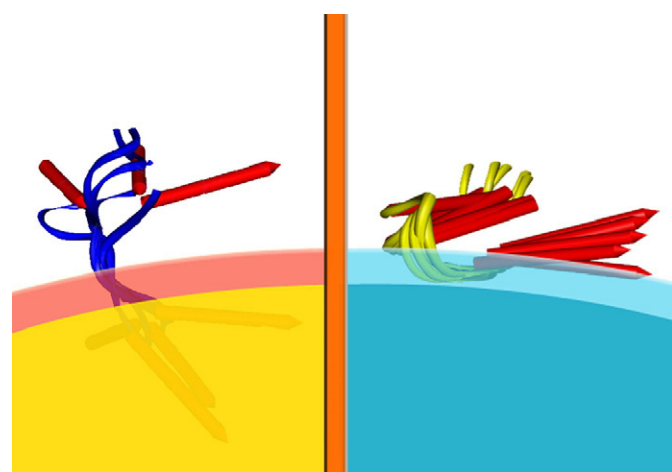


Fig. 7. Schematic representation of A β (16–35) orientation on SDS (left) and DPC/SDS (right) micelles. The portion of A β (16–35) spanning from the middle to the C-terminus is partially embedded in SDS micelles (left). Embedding of A β (16–35) is reduced in DPC/SDS, (right).

The reduction of the label mobility is a clear evidence of the insertion of the peptide, or of a segment of it, into the micellar core, since the local structuring of the alkyl chain tends to be more ordered in proximity of a guest molecule [88]. In contrast, the spectra of both spin labels in DPC/SDS mixed micelles were almost unaffected by the presence of A β (16–35), indicating no significant insertion of the peptide into the micelle interior. Thus, evidences obtained using spin-labeled lipids are in perfect agreement with those obtained with spin-labeled peptides, and support the peptide–micelle relative positioning proposed in Fig. 7.

To confirm EPR data, NMR experiments were recorded in micellar solutions containing 5-DSA or 16-DSA. Paramagnetic probes are able to induce a broadening of the NMR signals and a decrease in resonance intensities. Generally, the sites of the peptide which are close to the NO moiety are affected by the unpaired electrons with an increase in nuclear relaxation rates and, thus, a decrease in proton signals. If the peptide is close to the surface or penetrates the inner core of the micelle, a decrease in intensity is observed in 5-DSA spin-labeled micelles or in 16 DSA spin-labeled micelles, respectively [59]. 1D and 2D TOCSY spectra of the A β (16–35) were recorded in pure SDS micelles in the presence and absence of 5-DSA and 16-DSA, keeping all other conditions constant. A comparison of TOCSY spectra shows an unspecific modification of CH α -NH cross peaks when A β (16–35) was solved in DPC/SDS micelles containing 5-DSA or 16-DSA. In SDS micelles, a selective perturbation of CH α -NH TOCSY signals were observed in the presence of 5-DSA spin labels, where a decrease of signals relative to K28–M35 residues was evident.

4. Discussion

A great deal of evidence implicates the plasma membrane in processes leading to the misfolding and aggregation of β -amyloid peptides. Accordingly, A β peptides have been extensively analyzed in membrane-mimicking systems that are characterized by different complexities and compositions.

Although all evidence shows that membrane charge is a critical factor in modulating the conformational behavior of amyloid peptides, the exact definition for the role of charge in affecting conformations of amyloid peptide is controversial. Some data suggest that net negative charge is essential in favoring the presence of peptide monomers. Some others indicate that negatively charged membranes could catalyze the transition of A β peptide to β -conformation and aggregation [17–20,22,40].

Micellar aggregates are extremely simplified models of biological membranes. Nevertheless, they offer the advantage of enabling high-resolution NMR solution studies. This is thanks to the rapid and effectively isotropic reorientation of the protein [47].

High-resolution structures of A β peptide, in strongly negative charged SDS micelles and in zwitterionic DPC micelles, have been solved using NMR spectroscopy [41–46]. Mixtures of DPC “doped” with small amounts of SDS may be used to modulate the charge distribution of the micelle surface.

In the present work we probed the conformational behavior of A β (16–35) in response to negative charge modifications of the micelle surface. Toward this end, we performed solution spectroscopic studies of the amyloid fragment A β (16–35) in pure SDS micelles and in mixed DPC/SDS 90/10 w:w micelles.

A β (16–35) represents the hydrophobic central part of β -amyloid peptide, being implicated in aggregation/disaggregation processes. In fibril structural models, [15] it represents the repetitive unit of β -amyloid peptide aggregates. In a recent search for amyloid antibodies, this fragment was found to be specifically linked to antibodies [16]. In spite of the numerous structural studies made on several different fragments of β -amyloid peptides [41–46] with the exception of a computational study that demonstrated the structural importance of a salt bridge between D23 and K28, [89] data on the A β (16–35) structure has not been available until now.

Results presented here show that A β (16–35) in SDS micelles assumed regular α -helical and type I β -turn conformations involving the residues L17–D23 and G29–L34, respectively. Segment V24–K28 was highly flexible, as evidenced by scattering of the dihedral angles of residues G25 and S26. Thus, the two turn-helical pieces were free to vary their reciprocal orientation. Addition of zwitterionic surfactant to produce DPC/SDS mixed micelles, induced a decrease in L17–D23 and G29–M35 structural regularity and a tightening of the V24–K28 segment. Most of the A β (16–35) NMR structures in DPC/SDS micelles were characterized by regular type I β -turns in V24–K28. From this portion, regular turn structures alternatively span the N- or C-terminus of the peptide.

Previous conformational studies have shown that amyloid peptides in SDS micelles [41–43] and in water/fluorinated solvent mixtures [90,91] exhibit N and C-terminal turn-helical structures. Their reciprocal orientation is regulated by the flexible kink of V24–K28. On the other hand, according to computational models [89] of A β (16–35), solid-state NMR analyses for A β (9–40) peptides [92], and H–D exchange NMR-based A β (17–42) protofibril structures, [15] amyloid peptides in the protofibril are organized in two ordered β -strands, with a connecting loop having an intramolecular salt bridge between residues D23 and K28. Remarkably, both computational and experimental models agree that the structure has a U-turn shape, even if each model proposes a distinct structure for the turn. Currently there is increasing evidence [93–95] that the U-shaped ‘ β -strand–loop– β -strand’ motif observed in the A β organization is generally applicable to all amyloids, including β_2 -microglobulin [94] and human

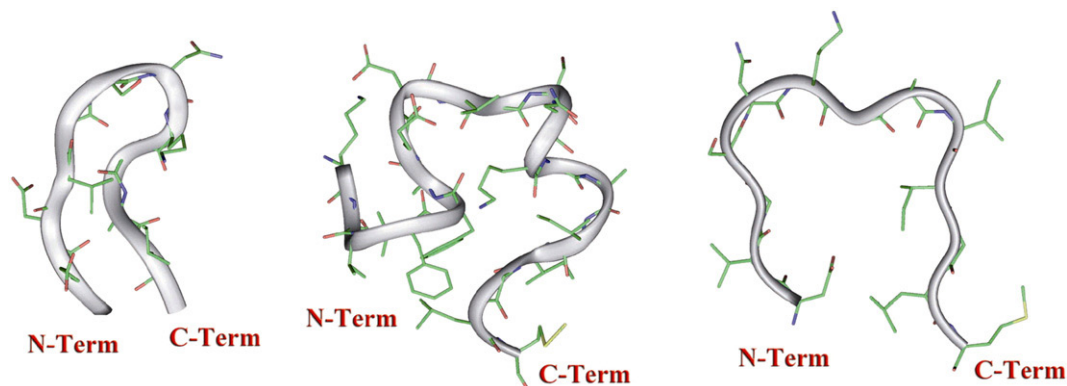


Fig. 8. U-turn shaped structural motif of A β (16–35) in DPC/SDS mixed micelles (centre) as compared to U-turn shaped A β (1–40) affibody-complex (left) (Hoyer et al. 2008; PDB id: 2OTK) and A β (1–40) in protofibril models (right) (Luhers et al. 2005; PDB id: 2BEG).

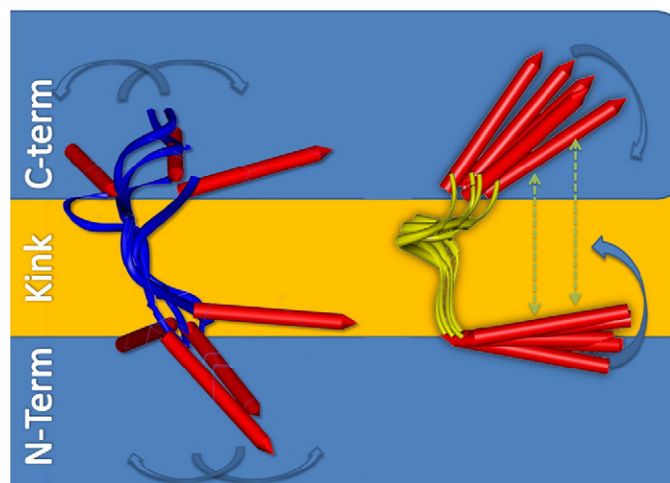


Fig. 9. Schematic representation of A β (16–35) conformational transition from helical-kink-helical structure, to U-Turn shaped conformation resembling protofibril models.

cancer antigen 150 (CA150) [93]. Finally, recently the determination of the structure of A β (1–40) complexed to an Az3 affibody was carried out [16]. This demonstrated that the portion of A β (1–40) that is linked to the affibody protein corresponds to an A β (16–35) fragment and is arranged in a β -hairpin structure.

The structure of A β (16–35) in SDS micelles, as found in the present work, resembles others solved in the same conditions. Consistently, we observed high solubility and structural organization. In SDS micelles, a helix–turn–helix was found with high flexibility of kink peptide. Here the regularity of the conformations at the N and C-terminus and the flexibility of the hinge guarantee the solubility of the fragment and stabilization of peptide monomers.

A β (16–35) in DPC/SDS micelles exhibited the U-turn shaped structural motif that has been observed in protofibril models and is typical of all amyloid conformations (Fig. 8) [93–95]. In these conditions, the structural compactness of C- and N-terminal helices was lost and the tightening of the ²⁴VGSNK²⁸ kink segment favored intramolecular and intermolecular contacts. This potentially could lead to aggregation through inter-stands, with intermolecular contacts between. In a similar manner to the conformation of the A β (1–40) affibody-complex, this is an example of an A β fragment in soluble form that has the U-turn shape of protofibrils.

Results derived from EPR experiments using MTSL spin-labeled peptide provided additional elements to interpret our conformational findings. Spin-label aided experiments demonstrated that the portion of A β (16–35) spanning from the middle to the C-terminus was partially embedded in SDS micelles (see Fig. 7). This effect can be promoted by the electrostatic attraction mediated via the positively charged 28 K with the sulphate of the surfactants. In these conditions, the salt bridge between D23 and K28 – which is considered a structural peculiarity of A β peptides in fibril models- and consequently the spatial contacts between the two termini are hampered. On the contrary, in DPC/SDS, a minor electrostatic attraction is plausible. Thus, embedding of the peptide in the micelle interior is reduced and the intramolecular and possibly intermolecular interactions between the C- and N-terminal segments are favored.

Interestingly EPR spectra revealed a higher increase in correlation time, i.e., a stronger reduction of the label rotational mobility, for A β (16–35)G25C-MTSL in DPC/SDS mixed micelles. This evidence, together with the decrease in flexibility observed for A β (16–35) in DPC/SDS, depicts a conformational state that may be preliminary to aggregation. (Fig. 9).

Thus, we speculated that the conformations in DPC/SDS presented here constitute intermediate conformations on the pathway to amyloid fibrils. Decreasing charge results in tightening of the V24–

K28 kink, and the concomitant destabilization of turn-helical pieces. These events are strategic to move toward a strand–turn–strand conformation, which is the milestone of amyloid aggregates.

The poor solubility of amyloid aggregates in the media normally used for the biological tests hampers an extensive experimentation of molecules potentially active as preventing and/or reversing of fibril aggregation. Interestingly our structure in DPC/SDS micelle can be viewed as soluble form of U-turn shaped β -amyloid protofibrils, that can be a promising target to test new anti-Alzheimer agents.

Appendix A. Supplementary data

Supplementary data associated with this article can be found, in the online version, at doi:10.1016/j.bbamem.2009.12.012.

References

- [1] D.J. Selkoe, Alzheimer's disease: genes, proteins, and therapy, *Physiol. Rev.* 81 (2001) 741–766.
- [2] D.M. Walsh, D.J. Selkoe, Deciphering the molecular basis of memory failure in Alzheimer's disease, *Neuron* 44 (2004) 181–193.
- [3] J.D. Sipe, A.S. Cohen, Review: history of the amyloid fibril, *J. Struct. Biol.* 130 (2000) 88–98.
- [4] J. Hardy, D.J. Selkoe, The amyloid hypothesis of Alzheimer's disease: progress and problems on the road to therapeutics, *Science* 297 (2002) 353–356.
- [5] L. Haataja, T. Gurlo, C.J. Huang, P.C. Butler, Islet amyloid in type 2 diabetes, and the toxic oligomer hypothesis, *Endocr. Rev.* 29 (2008) 303–316.
- [6] P.A. Temussi, L. Masino, A. Pastore, From Alzheimer to Huntington: why is a structural understanding so difficult? *EMBO J.* 22 (2003) 355–361.
- [7] D.J. Selkoe, Translating cell biology into therapeutic advances in Alzheimer's disease, *Nature* 399 (1999) A23–A31.
- [8] L.L. Iversen, R.J. Mortishire-Smith, S.J. Pollack, M.S. Shearman, The toxicity in vitro of beta-amyloid protein, *Biochem. J.* 311 (Pt 1) (1995) 1–16.
- [9] D.A. Kirschner, C. Abraham, D.J. Selkoe, X-ray diffraction from intraneuronal paired helical filaments and extraneuronal amyloid fibers in Alzheimer disease indicates cross-beta conformation, *Proc. Natl. Acad. Sci. U. S. A.* 83 (1986) 503–507.
- [10] C. Soto, E.M. Castano, B. Frangione, N.C. Inestrosa, The alpha-helical to beta-strand transition in the amino-terminal fragment of the amyloid beta-peptide modulates amyloid formation, *J. Biol. Chem.* 270 (1995) 3063–3067.
- [11] J. McLaurin, D. Yang, C.M. Yip, P.E. Fraser, Review: modulating factors in amyloid-beta fibril formation, *J. Struct. Biol.* 130 (2000) 259–270.
- [12] K.L. Sciarretta, D.J. Gordon, S.C. Meredith, Peptide-based inhibitors of amyloid assembly, *Methods Enzymol.* 413 (2006) 273–312.
- [13] C. Soto, E.M. Sigurdsson, L. Morelli, R.A. Kumar, E.M. Castano, B. Frangione, Beta-sheet breaker peptides inhibit fibrillogenesis in a rat brain model of amyloidosis: implications for Alzheimer's therapy, *Nat. Med.* 4 (1998) 822–826.
- [14] L.O. Tjernberg, J. Naslund, F. Lindqvist, J. Johansson, A.R. Karlstrom, J. Thyberg, L. Terenius, C. Nordstedt, Arrest of beta-amyloid fibril formation by a pentapeptide ligand, *J. Biol. Chem.* 271 (1996) 8545–8548.
- [15] T. Luhrs, C. Ritter, M. Adrian, D. Riek-Loher, B. Bohrmann, H. Dobeli, D. Schubert, R. Riek, 3D structure of Alzheimer's amyloid-beta(1–42) fibrils, *Proc. Natl. Acad. Sci. U. S. A.* 102 (2005) 17342–17347.
- [16] W. Hoyer, C. Grönwall, A. Jonsson, S. Stahl, T. Härd, Stabilization of a -hairpin in monomeric Alzheimer's amyloid- peptide inhibits amyloid formation, *Proc. Natl. Acad. Sci.* 105 (2008) 5099.
- [17] G.P. Gorbenko, P.K. Kinnunen, The role of lipid-protein interactions in amyloid-type protein fibril formation, *Chem. Phys. Lipids* 141 (2006) 72–82.
- [18] A.T. Alexandrescu, Amyloid accomplices and enforcers, *Protein Sci.* 14 (2005) 1–12.
- [19] J.D. Harper, P.T. Lansbury Jr., Models of amyloid seeding in Alzheimer's disease and scrapie: mechanistic truths and physiological consequences of the time-dependent solubility of amyloid proteins, *Annu. Rev. Biochem.* 66 (1997) 385–407.
- [20] P. Hortschansky, V. Schroeckh, T. Christopeit, G. Zandomenighi, M. Fandrich, The aggregation kinetics of Alzheimer's beta-amyloid peptide is controlled by stochastic nucleation, *Protein Sci.* 14 (2005) 1753–1759.
- [21] R. Nanga, J. Brender, J. Xu, K. Hartman, V. Subramanian, A. Ramamoorthy, Three-dimensional structure and orientation of rat islet amyloid polypeptide protein in a membrane environment by solution NMR spectroscopy, *J. Am. Chem. Soc.* 131 (2009) 8252–8261.
- [22] C. Haass, D.J. Selkoe, Soluble protein oligomers in neurodegeneration: lessons from the Alzheimer's amyloid beta-peptide, *Nat. Rev. Mol. Cell. Biol.* 8 (2007) 101–112.
- [23] J. Brender, E. Lee, M. Cavitt, A. Gafni, D. Steel, A. Ramamoorthy, Amyloid fiber formation and membrane disruption are separate processes localized in two distinct regions of IAPP, the type-2-diabetes-related peptide, *J. Am. Chem. Soc.* 130 (2008) 6424–6429.
- [24] R. Nanga, J. Brender, J. Xu, G. Veglia, A. Ramamoorthy, Structures of rat and human islet amyloid polypeptide IAPP1–19 in micelles by NMR spectroscopy, *Biochemistry* 47 (2008) 12689–12697.
- [25] J. Brender, K. Hartman, K. Reid, R. Kennedy, A. Ramamoorthy, A single mutation in the nonamyloidogenic region of islet amyloid polypeptide greatly reduces toxicity, *Biochemistry* 47 (2008) 12680–12688.

- [26] F.M. LaFerla, Calcium dyshomeostasis and intracellular signalling in Alzheimer's disease, *Nat. Rev. Neurosci.* 3 (2002) 862–872.
- [27] M.P. Mattson, Pathways towards and away from Alzheimer's disease, *Nature* 430 (2004) 631–639.
- [28] D.J. Selkoe, Developing preventive therapies for chronic diseases: lessons learned from Alzheimer's disease, *Nutr. Rev.* 65 (2007) S239–S243.
- [29] P. Smith, J. Brender, A. Ramamoorthy, Induction of negative curvature as a mechanism of cell toxicity by amyloidogenic peptides: the case of islet amyloid polypeptide, *J. Am. Chem. Soc.* 131 (2009) 4470–4478.
- [30] S.T. Ferreira, M.N. Vieira, F.G. De Felice, Soluble protein oligomers as emerging toxins in Alzheimer's and other amyloid diseases, *IUBMB Life* 59 (2007) 332–345.
- [31] R. Soong, J. Brender, P. Macdonald, A. Ramamoorthy, Association of highly compact type II diabetes related islet amyloid polypeptide intermediate species at physiological temperature revealed by diffusion NMR spectroscopy, *J. Am. Chem. Soc.* 131 (2009) 7079–7085.
- [32] J. McLaurin, A. Chakrabarty, Characterization of the interactions of Alzheimer beta-amyloid peptides with phospholipid membranes, *Eur. J. Biochem.* 245 (1997) 355–363.
- [33] F. Lindström, M. Bokvist, T. Sparman, G. Gröbner, Association of amyloid-peptide with membrane surfaces monitored by solid state NMR, *Phys. Chem. Chem. Phys.* 4 (2002) 5524–5530.
- [34] M. Bokvist, F. Lindström, A. Watts, G. Gröbner, Two types of Alzheimer's beta-amyloid (1–40) peptide membrane interactions: aggregation preventing transmembrane anchoring versus accelerated surface fibril formation, *J. Mol. Biol.* 335 (2004) 1039–1049.
- [35] J. Brender, U. Dürr, D. Heyl, M. Budarapu, A. Ramamoorthy, Membrane fragmentation by an amyloidogenic fragment of human islet amyloid polypeptide detected by solid-state NMR spectroscopy of membrane nanotubes, *BBA-Biomembranes* 1768 (2007) 2026–2029.
- [36] J.J. Kremer, M.M. Pallitto, D.J. Sklansky, R.M. Murphy, Correlation of beta-amyloid aggregate size and hydrophobicity with decreased bilayer fluidity of model membranes, *Biochemistry* 39 (2000) 10309–10318.
- [37] C. Ege, J. Majewski, G. Wu, K. Kjaer, K.Y. Lee, Templating effect of lipid membranes on Alzheimer's amyloid beta peptide, *Chemphyschem* 6 (2005) 226–229.
- [38] E. Maltseva, A. Kerth, A. Blume, H. Mohwald, G. Brezesinski, Adsorption of amyloid beta (1–40) peptide at phospholipid monolayers, *Chembiochem* 6 (2005) 1817–1824.
- [39] C. Ege, K.Y. Lee, Insertion of Alzheimer's A beta 40 peptide into lipid monolayers, *Biophys. J.* 87 (2004) 1732–1740.
- [40] A. Naito, I. Kawamura, Solid-state NMR as a method to reveal structure and membrane-interaction of amyloidogenic proteins and peptides, *BBA-Biomembranes* 1768 (2007) 1900–1912.
- [41] M. Coles, W. Bicknell, A. Watson, D. Fairlie, D. Craik, Solution structure of amyloid beta-peptide (1–40) in a water-micelle environment. Is the membrane-spanning domain where we think it is, *Biochemistry* 37 (1998) 11064–11077.
- [42] H. Shao, S. Jao, K. Ma, M.G. Zagorski, Solution structures of micelle-bound amyloid beta-(1–40) and beta-(1–42) peptides of Alzheimer's disease, *J. Mol. Biol.* 285 (1999) 755–773.
- [43] J. Jarvet, J. Danielsson, P. Damberg, M. Oleszczuk, A. Graslund, Positioning of the Alzheimer Aβeta(1–40) peptide in SDS micelles using NMR and paramagnetic probes, *J. Biomol. NMR* 39 (2007) 63–72.
- [44] J. Talafous, K.J. Marciniowski, G. Klopman, M.G. Zagorski, Solution structure of residues 1–28 of the amyloid beta-peptide, *Biochemistry* 33 (1994) 7788–7796.
- [45] T. Kohno, K. Kobayashi, T. Maeda, K. Sato, A. Takashima, Three-dimensional structures of the amyloid beta peptide (25–35) in membrane-mimicking environment, *Biochemistry* 35 (1996) 16094–16104.
- [46] T.G. Fletcher, D.A. Keire, The interaction of beta-amyloid protein fragment (12–28) with lipid environments, *Protein Sci.* 6 (1997) 666–675.
- [47] C. Mateo, J. Gómez, J. Villalain, J. González-Ros, Protein-lipid interactions: new approaches and emerging concepts, Springer, 2006.
- [48] G. Henry, B. Sykes, Methods to study membrane protein structure in solution, *Methods Enzymol.* 239 (1994) 515.
- [49] G. Privé, Detergents for the stabilization and crystallization of membrane proteins, *Methods* 41 (2007) 388–397.
- [50] F. Porcelli, B.A. Buck-Koehntop, S. Thennarasu, A. Ramamoorthy, G. Veglia, Structures of the dimeric and monomeric variants of magainin antimicrobial peptides (MSI-78 and MSI-594) in micelles and bilayers, determined by NMR spectroscopy, *Biochemistry* 45 (2006) 5793–5799.
- [51] F. Porcelli, R. Verardi, L. Shi, K.A. Henzler-Wildman, A. Ramamoorthy, G. Veglia, NMR structure of the cathelicidin-derived human antimicrobial peptide LL-37 in dodecylphosphocholine micelles, *Biochemistry* 47 (2008) 5565–5572.
- [52] A. Rath, M. Glibowicka, V. Nadeau, G. Chen, C. Deber, Detergent binding explains anomalous SDS-PAGE migration of membrane proteins, *Proc. Natl. Acad. Sci.* 106 (2009) 1760.
- [53] P. Somasundaran, S. Staff, *Encyclopedia of surface and colloid science*, CRC Press, 2006.
- [54] P. Gorman, S. Kim, M. Guo, R. Melnyk, J. McLaurin, P. Fraser, J. Bowie, A. Chakrabarty, Dimerization of the transmembrane domain of amyloid precursor proteins and familial Alzheimer's disease mutants, *BMC Neurosci.* 9 (2008) 17.
- [55] J.H. Chill, J.M. Louis, C. Miller, A. Bax, NMR study of the tetrameric KcsA potassium channel in detergent micelles, *Protein Sci.* 15 (2006) 684–698.
- [56] M.P. Williamson, Y. Suzuki, N.T. Bourne, T. Asakura, Binding of amyloid beta-peptide to ganglioside micelles is dependent on histidine-13, *Biochem. J.* 397 (2006) 483–490.
- [57] P. Mandal, J. Pettigrew, Alzheimer's disease: NMR studies of asialo (GM1) and trisialo (GT1b) ganglioside interactions with A (1–40) peptide in a membrane mimic environment, *Neurochem. Res.* 29 (2004) 447–453.
- [58] S. Rodziewicz-Motowidlo, P. Juszczyk, A.S. Kolodziejczyk, E. Sikorska, A. Skwierawska, M. Oleszczuk, Z. Grzonka, Conformational solution studies of the SDS micelle-bound 11–28 fragment of two Alzheimer's beta-amyloid variants (E22K and A21G) using CD, NMR, and MD techniques, *Biopolymers* 87 (2007) 23–39.
- [59] O. Zerbe, R. Mannhold, H. Kubinyi, G. Folkers, *BioNMR in drug research*, Vch Verlagsgesellschaft MbH, 2003.
- [60] L. Berliner, J. Reuben, *Spin labeling: theory and applications*, 1976.
- [61] J. Powell, E. II, P. Gannett, Improvement of a critical intermediate step in the synthesis of a nitroxide-based spin-labeled deoxythymidine analog, *Molecules* 5 (2000) 1244–1250.
- [62] H. Hankovszky, K. Hideg, L. Lex, Nitroxyls; VII. Synthesis and reactions of highly reactive 1-oxy-2, 2, 5, 5-tetramethyl-2, 5-dihydropyrrole-3-ylmethyl sulfonates, *Synthesis* (1980) 914–916.
- [63] D. Mustafa, A. Sosa-Peinado, V. Gupta, D. Gordon, M. Makinen, Structure of spin-labeled methylmethanethiolsulfonate in solution and bound to TEM-1 [beta]-lactamase determined by electron nuclear double resonance spectroscopy, *Biochemistry* 41 (2002) 797–808.
- [64] A. Shafer, T. Kalai, S. Liu, K. Hideg, J. Voss, Site-specific insertion of spin-labeled l-amino acids in xenopus oocytes, *Biochemistry* 43 (2004) 8470–8482.
- [65] W. Chan, P. White, *Fmoc Solid Phase Peptide Synthesis: A Practical Approach*, Oxford University Press, New York, 2000.
- [66] C.B. Karim, Z. Zhang, D.D. Thomas, Synthesis of TOAC spin-labeled proteins and reconstitution in lipid membranes, *Nat. Protoc.* 2 (2007) 42–49.
- [67] S. Jao, K. Ma, J. Talafous, R. Orlando, M. Zagorski, Trifluoroacetic acid pretreatment reproducibly disaggregates the amyloid β-peptide, *Amyloid* 4 (1997) 240–252.
- [68] M. Pellegrini, D.F. Mierke, Structural characterization of peptide hormone/receptor interactions by NMR spectroscopy, *Biopolymers* 51 (1999) 208–220.
- [69] K. Weller, S. Lauber, M. Lerch, A. Renaud, H.P. Merkle, O. Zerbe, Biophysical and biological studies of end-group-modified derivatives of Pep-1, *Biochemistry* 44 (2005) 15799–15811.
- [70] L. Whitmore, B. Wallace, DICHROWEB, an online server for protein secondary structure analyses from circular dichroism spectroscopic data, *Nucleic Acids Res.* 32 (2004) W668.
- [71] L. Wesson, D. Eisenberg, Atomic solvation parameters applied to molecular dynamics of proteins in solution, *Protein Sci.* 1 (1992).
- [72] U. Piantini, O. Sorensen, R. Ernst, Multiple quantum filters for elucidating NMR coupling networks, *J. Am. Chem. Soc.* 104 (1982) 6800–6801.
- [73] A. Bax, D. Davis, MLEV-17-based two-dimensional homonuclear magnetization transfer spectroscopy, *J. Magn. Res.* 65 (1985) 355–360.
- [74] J. Jeener, B. Meier, P. Bachmann, R. Ernst, Investigation of exchange processes by two-dimensional NMR spectroscopy, *J. Chem. Phys.* 71 (1979) 4546.
- [75] T. Goddard, D. Kneller, SPARKY 3 software, University of California, San Francisco, USA, 2006.
- [76] P. Guntert, C. Mumenthaler, K. Wuthrich, Torsion angle dynamics for NMR structure calculation with the new program DYANA, *J. Mol. Biol.* 273 (1997) 283–298.
- [77] D. Pearlman, D. Case, J. Caldwell, W. Ross, T. Cheatham III, S. DeBolt, D. Ferguson, G. Seibel, P. Kollman, Amber, a computer program for applying molecular mechanics, normal mode analysis, molecular dynamics and free energy calculations to elucidate the structures and energies of molecules, *Comp. Phys. Commun.* 91 (1995) 1–41.
- [78] D. Case, D. Pearlman, J. Caldwell, T. Cheatham III, W. Ross, C. Simmerling, T. Darden, K. Merz, R. Stanton, A. Cheng, AMBER 5.0, University of California, San Francisco, 1997.
- [79] K. Wüthrich, *NMR of Proteins and Nucleic Acids*, Wiley-Interscience, 1986.
- [80] D.S. Wishart, B.D. Sykes, F.M. Richards, The chemical shift index: a fast and simple method for the assignment of protein secondary structure through NMR spectroscopy, *Biochemistry* 31 (1992) 1647–1651.
- [81] R.A. Laskowski, J.A. Rullmann, M.W. MacArthur, R. Kaptein, J.M. Thornton, AQUA and PROCHECK-NMR: programs for checking the quality of protein structures solved by NMR, *J. Biomol. NMR* 8 (1996) 477–486.
- [82] J. Jarvet, J. Zdunek, P. Damberg, A. Graslund, Three-dimensional structure and position of porcine motilin in sodium dodecyl sulfate micelles determined by ¹H NMR, *Biochemistry* 36 (1997) 8153–8163.
- [83] M. Lindberg, J. Jarvet, U. Langel, A. Graslund, Secondary structure and position of the cell-penetrating peptide transportan in SDS micelles as determined by NMR, *Biochemistry* 40 (2001) 3141–3149.
- [84] A. Tedeschi, L. Franco, M. Ruzzi, L. Paduano, C. Corvaja, G. D'Errico, Micellar aggregation of alkyltrimethylammonium bromide surfactants studied by electron paramagnetic resonance of an anionic nitroxide, *Phys. Chem. Chem. Phys.* 5 (2003) 4204–4209.
- [85] C. Esposito, A. Tedeschi, M. Scrima, G. D'Errico, M.F. Ottaviani, P. Rovero, M. D'Ursi, A. Exploring interaction of beta-amyloid segment (25–35) with membrane models through paramagnetic probes, *J. Pept. Sci.* 12 (2006) 766–774.
- [86] D. Kivelson, Theory of ESR linewidths of free radicals, *J. Chem. Phys.* 33 (1960) 1094.
- [87] A. Tedeschi, G. D'Errico, E. Busi, R. Basosi, V. Barone, Micellar aggregation of sulfonate surfactants studied by electron paramagnetic resonance of a cationic nitroxide: an experimental and computational approach, *Phys. Chem. Chem. Phys.* 4 (2002) 2180–2188.
- [88] G. D'Errico, A. D'Ursi, D. Marsh, Interaction of a peptide derived from glycoprotein gp36 of feline immunodeficiency virus and its lipoylated analogue with phospholipid membranes, *Biochemistry* 47 (2008) 5317.
- [89] B. Ma, R. Nussinov, Molecular dynamics simulations of alanine rich -sheet oligomers: insight into amyloid formation, *Protein Science: A Publication of the Protein Society*, vol. 11, 2002, p. 2335.

- [90] O. Crescenzi, S. Tomaselli, R. Guerrini, S. Salvadori, A. D'Ursi, P. Temussi, D. Picone, Solution structure of the Alzheimer amyloid [beta]-peptide (1–42) in an apolar microenvironment: similarity with a virus fusion domain, *Eur. J. Biochem.* 269 (2002) 5642.
- [91] H. Sticht, P. Bayer, D. Willbold, S. Dames, C. Hilbich, K. Beyreuther, R.W. Frank, P. Rosch, Structure of amyloid A4-(1–40)-peptide of Alzheimer's disease, *Eur. J. Biochem.* 233 (1995) 293–298.
- [92] A.T. Petkova, W.M. Yau, R. Tycko, Experimental constraints on quaternary structure in Alzheimer's beta-amyloid fibrils, *Biochemistry* 45 (2006) 498–512.
- [93] N. Ferguson, J. Becker, H. Tidow, S. Tremmel, T.D. Sharpe, G. Krause, J. Flinders, M. Petrovich, J. Berriman, H. Oschkinat, A.R. Fersht, General structural motifs of amyloid protofilaments, *Proc. Natl. Acad. Sci. U. S. A.* 103 (2006) 16248–16253.
- [94] K. Iwata, T. Fujiwara, Y. Matsuki, H. Akutsu, S. Takahashi, H. Naiki, Y. Goto, 3D structure of amyloid protofilaments of beta2-microglobulin fragment probed by solid-state NMR, *Proc. Natl. Acad. Sci. U. S. A.* 103 (2006) 18119–18124.
- [95] J. Zheng, B. Ma, R. Nussinov, Consensus features in amyloid fibrils: sheet-sheet recognition via a (polar or nonpolar) zipper structure, *Phys. Biol.* 3 (2006) P1–P4.